

# Directionally selective calcium signals in dendrites of starburst amacrine cells

Thomas Euler\*, Peter B. Detwiler† & Winfried Denk\*

\* Max Planck Institute for Medical Research, Jahnstrasse 29, D-69120 Heidelberg, Germany

† University of Washington, Department of Physiology & Biophysics, Box 357290, Seattle, Washington 98195, USA

**The detection of image motion is fundamental to vision. In many species, unique classes of retinal ganglion cells selectively respond to visual stimuli that move in specific directions. It is not known which retinal cell first performs the neural computations that give rise to directional selectivity in the ganglion cell. A prominent candidate has been an interneuron called the ‘starburst amacrine cell’. Using two-photon optical recordings of intracellular calcium concentration, here we find that individual dendritic branches of starburst cells act as independent computation modules. Dendritic calcium signals, but not somatic membrane voltage, are directionally selective for stimuli that move centrifugally from the cell soma. This demonstrates that direction selectivity is computed locally in dendritic branches at a stage before ganglion cells.**

A substantial fraction of the neurons (retinal ganglion cells) that convey visual information out of the retina to the visual areas of the cerebral cortex respond with a strong spike discharge to a visual stimulus moving in a certain (preferred) direction but stay almost silent when the stimulus moves in the opposite (null) direction. They are therefore called ‘direction-selective (DS) ganglion cells’. Even though DS ganglion cells were first described nearly 40 years ago<sup>1</sup> the biophysical mechanism and cellular locus for direction discrimination have been debated ever since (reviewed in ref. 2).

One of the central questions has been whether motion direction is computed in the DS ganglion cell itself (postsynaptically), using synaptic inputs that are not direction-selective, or whether the crucial computational step occurs at an ‘earlier’ (presynaptic) point in the signal pathway, that is, in cells that provide synaptic input to DS ganglion cells. The leading candidate for such a presynaptic locus has long been the starburst amacrine cell<sup>3,4</sup>, a retinal interneuron with a highly symmetrical dendritic morphology, a peculiar distribution of inputs and outputs<sup>5</sup> (Fig. 1b), and an unusually high tiling overlap factor<sup>6</sup>.

The role of starburst cells in direction detection became controversial when experiments using a laser to ablate starburst cells seemed to rule out their essential participation in direction selectivity<sup>7</sup>. Subsequently, electrophysiological evidence was presented both in favour<sup>8</sup> of and against<sup>9</sup> direction selectivity being computed at a presynaptic locus. Finally, recent experiments showing that direction selectivity (tested in several different ways) is abolished by genetically targeted elimination of starburst cells<sup>10</sup> offer strong evidence that they are necessary for direction detection.

Starburst cells—like most retinal interneurons, but unlike interneurons in other parts of the central nervous system—are non-spiking. Like most amacrine cells, starburst cells possess no clear distinction between dendrite and axon, with synaptic outputs and inputs intermingled on neuronal processes (which are still called dendrites). Dendritic outputs allow locally computed information to be transferred to other cells without leaving any detectable signature in the electrical signal recorded from the soma<sup>11</sup>. To study locally computed signals it is, therefore, necessary to monitor dendritic activity directly using either electrical or optical recording techniques. In this work we have examined the role of starburst-cell dendrites in detecting the direction of moving stimuli by using two-photon fluorescence measurements to monitor dendritic signals evoked by visual stimuli.

## Optical recording in light-sensitive retina

Cells in the isolated intact rabbit retina were visualized with a two-photon laser scanning fluorescence microscope<sup>12</sup>. A schematic drawing of the set-up is shown in Fig. 1a. Cell bodies were visualized using sulphorhodamine in the bath solution as a counterstain<sup>13,14</sup>. We identified ‘ON’ starburst amacrine cells on the basis of their soma’s shape (circular, diameter ~10 μm), location in the ganglion cell layer and depolarizing electrical response to the onset of illumination. A cell was selected and impaled under fluorescence-imaging control with a sharp microelectrode. Membrane potential ( $V_m$ ) responses to visual stimuli were recorded and the cell was filled with fluorescent calcium indicator dye through the recording electrode, making it possible to visualize the full extent and fine structure of its neuronal morphology (Fig. 1b). The soma typically gives rise to 4–6 primary dendrites, which travel a short distance before dividing into a profusion of smaller branches with proximal, intermediate and distal zones<sup>5</sup>. The calcium dynamics in amacrine cells are particularly interesting because the output synapses in starburst cells are mainly restricted to the distal dendrites<sup>5,15</sup>, where numerous varicosities are also apparent (Fig. 1b).

Two-photon excitation allows fluorescence imaging while leaving the retina responsive to visual stimuli because the infrared laser light (at a wavelength of about 930 nm) is very poorly absorbed by photopigments. Microfluorimetry of indicator dyes can thus be used to study light-evoked changes of the cytosolic calcium concentration ( $[Ca^{2+}]$ ) in dendrites in the inner retina<sup>16</sup>. Figure 1c shows an example of the light-flash-triggered increase in fluorescence in a small region of a starburst-cell distal dendrite. Fluorescence intensity changes, reflecting changes in intracellular  $[Ca^{2+}]$ , could be evoked by visual stimuli, but also occurred spontaneously during uniform but constant illumination. Figure 1d shows examples of such spontaneous events recorded simultaneously from neighbouring dendritic branches.  $[Ca^{2+}]$  transients appeared to be uncorrelated at the two optical recording sites; an early indication that dendrites can act independently of each other. The traces in Fig. 1d also demonstrate that spontaneous events can be either slow or rapid transients. The kinetics of the fast events are reminiscent of large spontaneous depolarizing potentials that are a common feature of electrical recordings from somata of starburst cells<sup>17–19</sup>.

The amplitude of the  $[Ca^{2+}]$  changes evoked by visual stimuli varied depending on the distance of the recording site from the soma (Fig. 1e). The changes in  $[Ca^{2+}]$  were small in the proximal and intermediate zones of the dendrite and large in the distal zone. In distal portions of the dendrites light triggered either large rapid

increases in  $[Ca^{2+}]$  (Fig. 1e and Fig. 2, right trace) or smaller slower decreases (see Fig. 3), depending on the stimulus location. Because synaptic vesicle exocytosis is calcium-dependent and most output synapses are located in the distal zone of starburst cell dendrites, our remaining  $[Ca^{2+}]$  measurements concentrated on that region.

**Localization of dendritic signals**

We investigated the receptive-field structure of voltage and  $[Ca^{2+}]$  responses using ‘pie-wedge’-shaped sector stimuli (see Methods and the drawings at the top of Fig. 2) designed to test the independence of responses in the different dendritic branches. Although voltage responses (Fig. 2a, bottom traces) at the soma were only weakly dependent on the angular location of the stimulus, as would be expected from the symmetry of the dendritic tree, calcium increases were evoked by central sector stimuli only if the illuminated area included the dendritic branch where the recording site was located (Fig. 2). Depending on the spatial extent of the dendritic branch, one or at most two sectors elicited a  $[Ca^{2+}]$  response at a particular recording site. This shows that, at least in terms of their  $[Ca^{2+}]$  response, different dendritic branches can react to light stimuli locally and independently of each other, as predicted by some starburst cell models<sup>20,21</sup>. The electrical responses evoked by sur-

round stimulation were inhibitory (Fig. 3a, bottom traces) and included in a few cases a delayed excitatory (OFF) response (data not shown), comparable to those described in patch-clamp voltage recordings<sup>19,22</sup>.  $[Ca^{2+}]$  transients were more variable between cells and between different recording sites in the same cell when stimulated with surround sectors. In most cases, illumination of the surround caused a small, slowly developing decrease in  $[Ca^{2+}]$  that was followed by a delayed (about 100–150 ms) recovery (Fig. 3a) and occasionally a strong overshoot at the termination of the stimulus (OFF response; Fig. 3b).  $[Ca^{2+}]$  decreases evoked by surround stimuli were not necessarily restricted to ipsilateral sectors but could be evoked at all stimulus orientations (Fig. 3b), confirming that the cells’ inhibitory input is less localized than its excitatory input<sup>19,22</sup>. The decrease in  $[Ca^{2+}]$  was not blocked by the GABA<sub>A</sub>-receptor antagonists bicuculline (Fig. 3c) and SR-95531 (data not shown), which implies that this decrease is mediated by a different inhibitory pathway—such as via the suppression of tonic input from bipolar cell terminals by GABA<sub>C</sub>-receptor-mediated presynaptic inhibition<sup>18,23–25</sup>.

**Dendritic responses to moving stimuli**

Having established that dendritic branches can act independently of

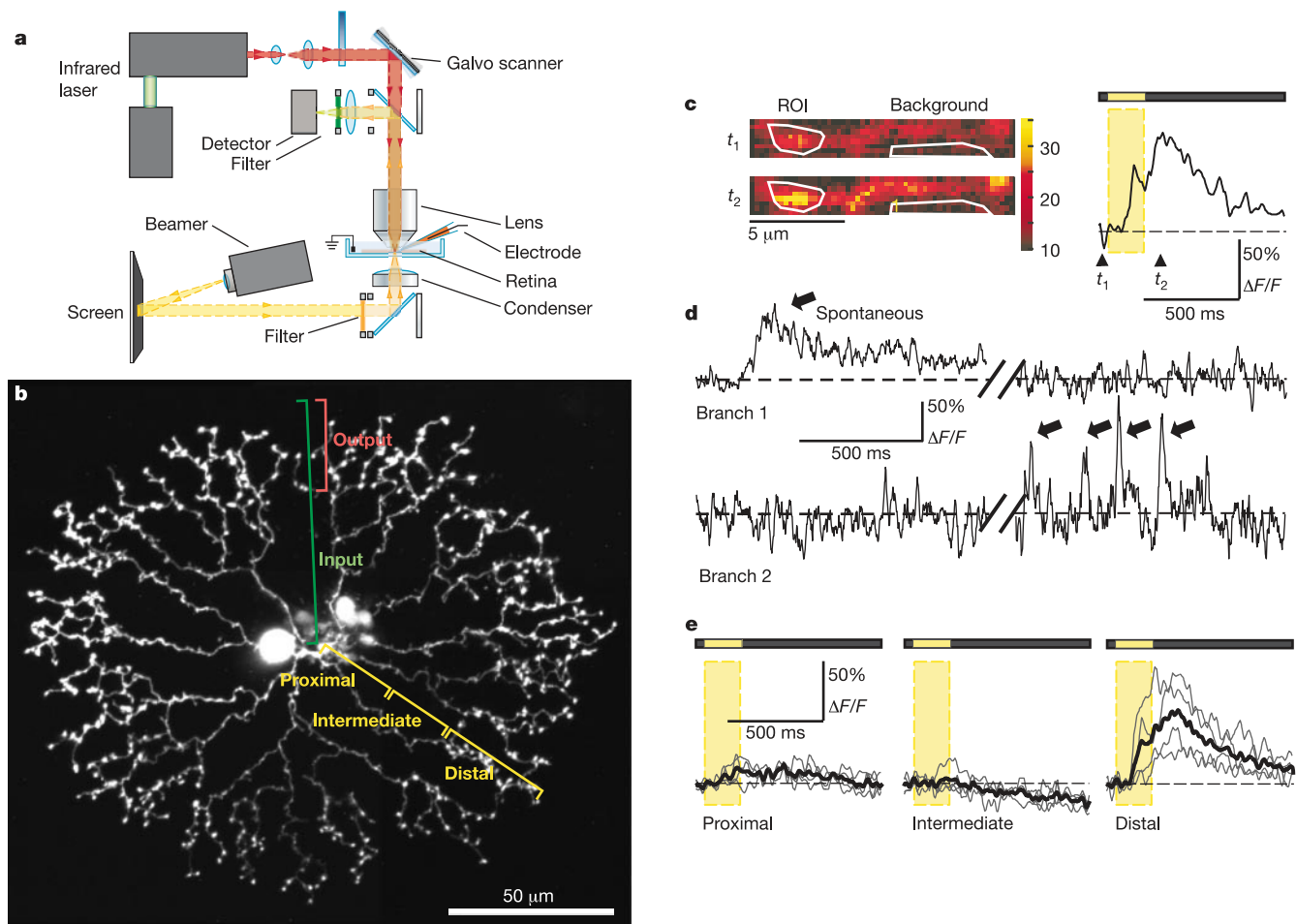


**Figure 1** Calcium responses in starburst amacrine cell dendrites. **a**, Two-photon laser scanning microscope with light stimulation and electrophysiological recording capabilities. **b**, ON starburst amacrine cell in a flat-mounted rabbit retina filled with Oregon Green BAPTA-1. **c**, Dendritic  $[Ca^{2+}]$  signals were monitored either with fast-frame scanning (c) or with line scans (not shown). The left panels (digitizer units) show a dendritic branch before ( $t_1$ ) and just after ( $t_2$ ) a light stimulus; the entire time course is

shown on the right (relative intensity change,  $\Delta F/F$ ) for the region of interest (ROI). The background area was used for baseline correction. Vertical yellow bar and yellow section of the bar above trace indicate stimulus duration. **d**, Spontaneous calcium events (arrows) with different timing and kinetics in neighbouring branches. **e**, Calcium signals evoked by stimuli flashed over dendrite recorded at three sites (13, 110 and 233  $\mu m$  from the soma) along the same branch.

each other we investigated whether individual branches can discriminate between different directions of image motion. The somatic voltage responded to moving stimuli but did so without any obvious directional preference (Fig. 4a–c). Its main characteristic is a modulation in synchrony with the changing local light level caused by the movement of the grating. In contrast, dendritic  $[Ca^{2+}]$  signals did show a strong directional dependence in response to both drifting gratings and moving bars (Fig. 4a, b, d). Grating movement in some directions triggered transient  $[Ca^{2+}]$  increases (Fig. 4a) that were modulated in synchrony with the light–dark periodicity of the stimulus. Movement of the grating in the opposite directions, however, had no effect on the intracellular  $[Ca^{2+}]$  at that recording location. The voltage and  $[Ca^{2+}]$  responses generated by moving bright bars (Fig. 4b) were more complex. The electrical response to moving bars (top traces in each pair) began with an initial hyperpolarization as the bar entered the cell’s surround (see icons at top). Next followed a depolarization as the bar moved over the cell’s dendritic tree and then again a hyperpolarization as the bar

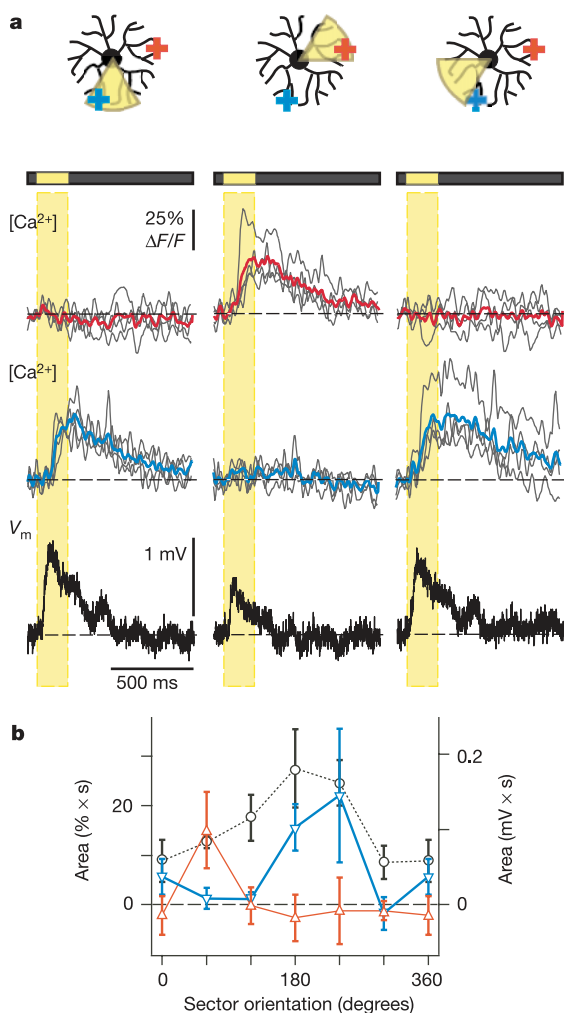


**Figure 2** Local stimulation evokes local calcium signals. Somatic voltage ( $V_m$ ) and dendritic  $[Ca^{2+}]$  in response to ‘pie-wedge’-shaped 60°-sector stimuli flashed for 200 ms in random order. In the icons the illuminated sector is shown in yellow; the black drawing represents the cell. Central sectors (a) always evoked depolarizations, but  $[Ca^{2+}]$  increases only when the recording site was illuminated; note recording sites (marked by red and blue crosses) on roughly opposite sides of the soma. Integrated  $[Ca^{2+}]$  responses (b) as a function of sector orientation for both recording sites (red and blue triangles) together with the electrical response (black circles). Error bars indicate s.d. ( $n = 4$ ).

moved off the cell into the near surround. Switching off the bar in the far surround (about 1.2 mm from the cell) evoked a brief depolarizing response, presumably reflecting the release of the strong and long-ranging inhibition that has been reported for these cells<sup>18</sup>. The  $[Ca^{2+}]$  response (bottom traces in each pair) began for all directions of motion as a slow, small depression later giving way to a recovery or even an increase above the resting  $[Ca^{2+}]$  that was largest when the bar moved in a particular direction over the optical recording site.

Closer analysis of the responses to moving stimuli shows how strong the calcium direction selectivity is. To quantify directional selectivity we temporally integrated voltage and  $[Ca^{2+}]$  changes (see

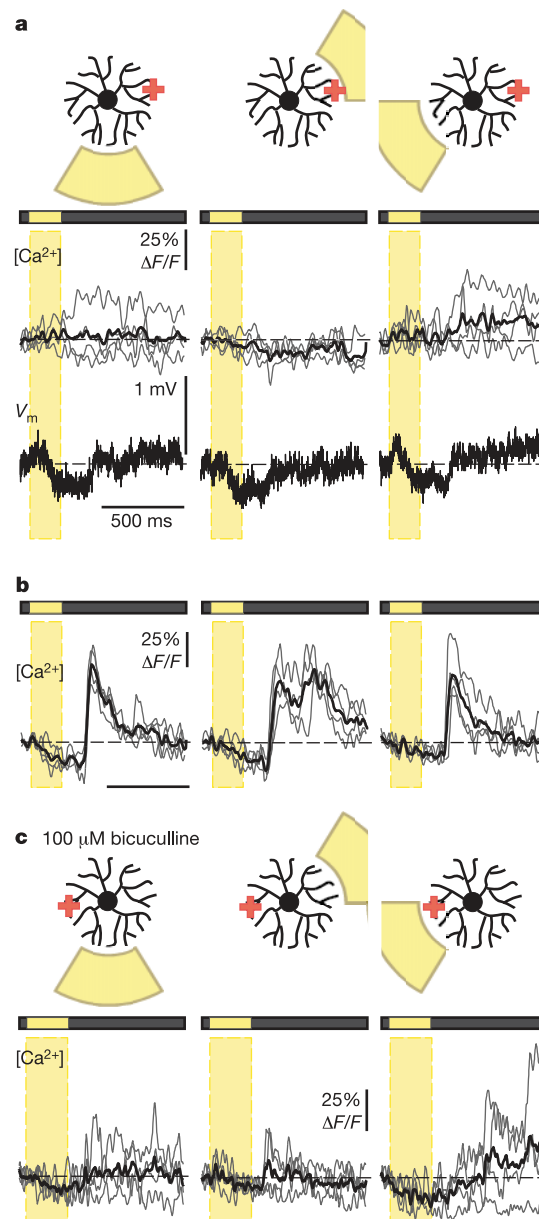


**Figure 3** Surround stimulation evokes a decrease in  $[Ca^{2+}]$  and occasionally transient increases after the end of the stimulus. Somatic voltage ( $V_m$ ) and dendritic  $[Ca^{2+}]$  in response to ‘pie-wedge’-shaped 60°-sector stimuli flashed for 200 ms (400 ms in c) over the receptive field surround.  $[Ca^{2+}]$  depression and hyperpolarization were almost always observed (a and b) but delayed  $[Ca^{2+}]$  increase after stimulus-offset occurred only occasionally (b). Neither the  $[Ca^{2+}]$  depression nor the delayed increase were abolished by the GABA<sub>A</sub> blocker bicuculline (c).

Methods) and plotted the results as a function of motion direction using polar coordinates (Fig. 4c, d). The normalized vector sum of the responses points in the preferred direction with its length providing a measure (the directional preference index, DPI; see Methods) of the strength of the motion-direction discrimination. Preferred direction and DPIs (for the responses shown in Fig. 4a–d) are represented by arrows (resultant vectors) originating at the approximate recording sites on a schematic starburst cell (Fig. 4e).

The DPIs for voltage ( $V_m$ ) and  $[Ca^{2+}]$  responses to a drifting grating were 0.09 and 0.67, respectively. The corresponding DPIs for the moving bar were 0.08 and 0.40. The histogram of DPIs for all cells tested is shown in Fig. 4f. The DPI values (mean  $\pm$  s.e.m) for all cells were  $0.18 \pm 0.02$  ( $n = 9$ ) and  $0.43 \pm 0.04$  ( $n = 12$ ) for  $V_m$  and dendritic  $[Ca^{2+}]$  responses, respectively.

We next analysed how the locally preferred direction relates to cellular morphology (Fig. 5). In most cases  $[Ca^{2+}]$  signals were

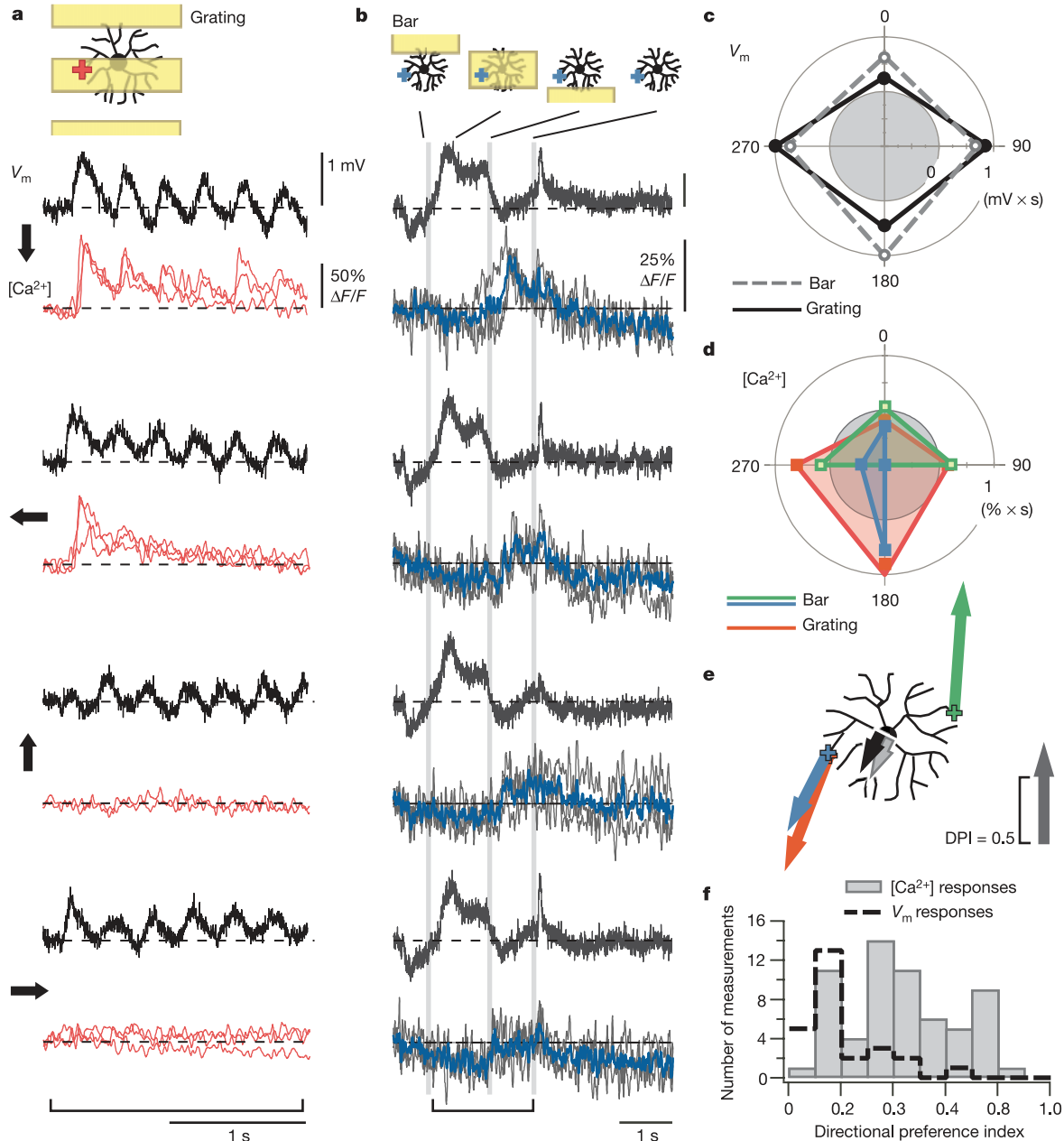


**Figure 4** Moving stimuli evoke direction-selective calcium responses in dendrites. Somatic voltage ( $V_m$ ) and dendritic  $[Ca^{2+}]$  responses of a starburst cell to moving gratings (a) and moving bars (b); averages of three trials. Direction of movement indicated by arrows next to each pair of traces. Stimulus speed was  $1.3 \text{ mm s}^{-1}$  for the grating (period,  $400 \mu\text{m}$ ; 82% contrast; mean intensity, about  $700 \text{ photons s}^{-1} \mu\text{m}^{-2}$ ) and  $1.0 \text{ mm s}^{-1}$  for the bar ( $500 \mu\text{m}$  wide; 87% contrast). The grating started moving 50 ms after the beginning of the traces (in a) and continued with constant velocity throughout the trace. Modulation of  $V_m$  (upper trace in each pair) did not depend strongly on motion direction either for the drifting grating (a) or for the moving bar (b).  $[Ca^{2+}]$  changes (lower trace in each pair) in distal dendritic segments occurred only when the grating moved towards

$180^\circ$  or  $270^\circ$  (a). The bar moving towards  $180^\circ$  caused the largest  $[Ca^{2+}]$  peak (b). Voltage (c) and  $[Ca^{2+}]$  (d) responses integrated over the stimulus duration (marked by bracket below traces in a and b) and plotted as function of the direction of motion. Green trace in polar plot represents bar responses for second recording site located on the opposite side of the cell (traces not shown). e, Arrows on schematic cell represent the directionality vector (v). DPI values for  $[Ca^{2+}]$  signals were 0.67 (red), 0.40 (blue), and 0.72 (green); for voltage responses 0.09 (black), and 0.08 (grey). Arrow origins indicate positions of recording sites. f, Histogram with DPI values for nine electrically recorded (dashed line; 26 measurements) and 12 optically recorded cells (62 measurements).



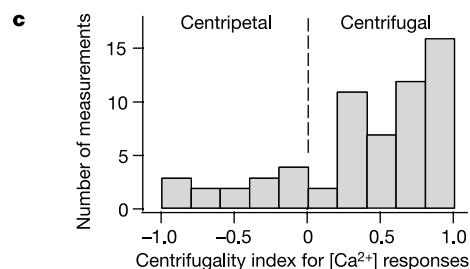
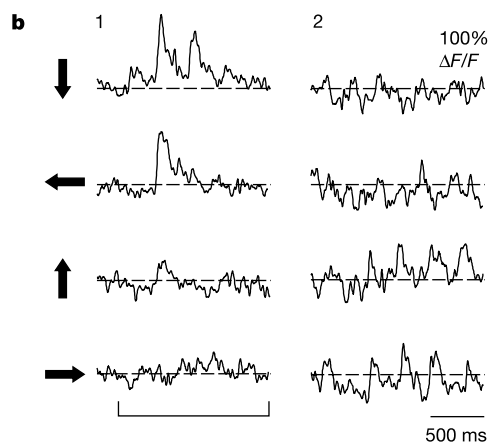
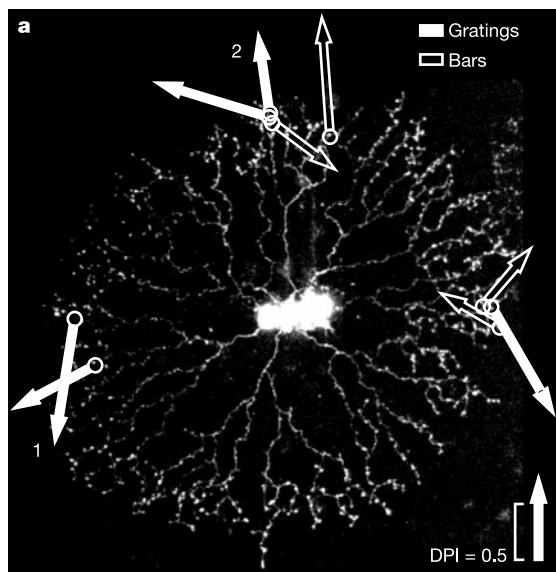


**Figure 5** Preferred direction and cellular morphology. **a**, Preferred direction and DPI probed by bars (open arrows) or gratings (solid arrows) for various dendritic locations (circles at arrow origins) in one starburst cell. **b**, For two recording sites (arrows marked 1 and 2) the time traces of the grating  $[Ca^{2+}]$  responses are shown. **c**, Distribution of centrifugality index (CI) values for all 12 cells tested (62 measurements).

larger for stimuli that moved outward from the soma, that is, for centrifugal directions of motion. This is apparent at several different recording sites for the cell in Fig. 5a. The directionality vectors at different dendritic sites did not, in general, point straight outward from the soma. We quantified the deviations from a strictly centrifugal line with a centrifugality index (CI) that ranged from +1 for perfect centrifugal preference to -1 for perfect centripetal preference (see Methods). For the cell in Fig. 5 the CI was  $0.43 \pm 0.18$  ( $n = 12$ ;  $DPI = 0.47 \pm 0.07$ ), indicating a clear preference for centrifugal motion; for all 12 cells tested the mean CI was  $0.42 \pm 0.06$  (see histogram in Fig. 5c).

Blocking  $GABA_A$  receptors abolishes direction selectivity in DS

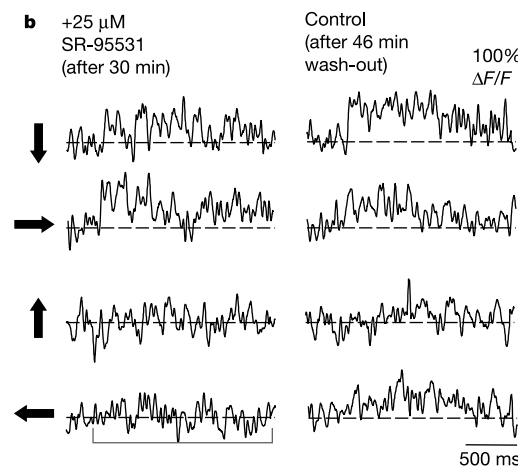
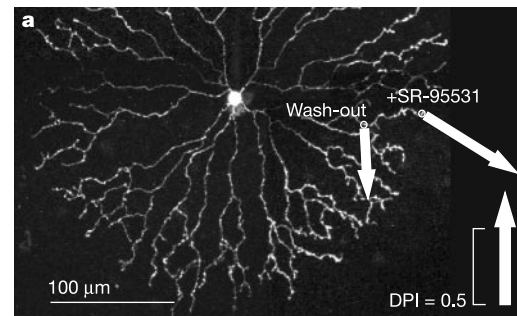


**Figure 6** The  $GABA_A$  blocker SR-95531 caused increased spontaneous activity but no reduction of  $[Ca^{2+}]$ -signal direction selectivity. **a**, **b**, DPIs of 0.61 and 0.32 under  $GABA_A$  block (**a**) and after wash-out (**b**).

ganglion cells<sup>25,26</sup> but not, as we found (Fig. 2c), the depression of  $[Ca^{2+}]$  by surround illumination, so we investigated the effect of  $GABA_A$  receptor antagonists on the  $[Ca^{2+}]$  responses to moving stimuli. We found that in the presence of either 100  $\mu M$  bicuculline or 20–50  $\mu M$  SR-95531 spontaneous activity increased, but evoked  $[Ca^{2+}]$  signals remained direction-selective ( $DPI = 0.53 \pm 0.04$ ;  $CI = 0.45 \pm 0.14$ ;  $n = 4$ ; Fig. 6a, b).

### Somatic responses to circular wave stimuli

The  $[Ca^{2+}]$  signals we have recorded show that dendritic sectors act as independent motion detectors with a direction of preference centrifugal from the soma. To test with somatic voltage recordings whether direction selectivity is also present in the electrical signal from each dendrite, we have to avoid cancellation of voltage contributions from different branches, which, for uniform motion, ‘see’ motion along preferred, neutral and null directions (depending on their orientation). Instead of uniform stimuli we therefore used expanding or contracting concentric waves (see Methods), which should excite each branch in the same sense. When comparing expanding and contracting stimuli we found very similar electrical responses (Fig. 7a), consisting of a net (direct current, d.c.) depolarization (expanding:  $0.31 \pm 0.07$  mV; contracting:  $0.42 \pm 0.06$  mV; ratios:  $0.73 \pm 0.16$ , range: 0.14 to 1.19;  $n = 6$ ; four cells) with a superimposed modulation (expanding:  $V_{rms} = 0.33 \pm 0.07$  mV; contracting:  $V_{rms} = 0.25 \pm 0.03$  mV; ratios:  $1.28 \pm 0.18$ , range: 0.89 to 2.02). The  $[Ca^{2+}]$  signals, on the other hand, were much larger for the expanding ( $21 \pm 7\% \Delta F/F$ ;  $n = 7$ ; six cells) than for the contracting stimulus ( $4 \pm 2\% \Delta F/F$ ). Although there was no clear difference in either the net (integrated) electrical depolarization or the modulation amplitude we wondered if underlying differences might have been masked by strong proximal bipolar cell input<sup>5</sup> driven by the modulation of the central

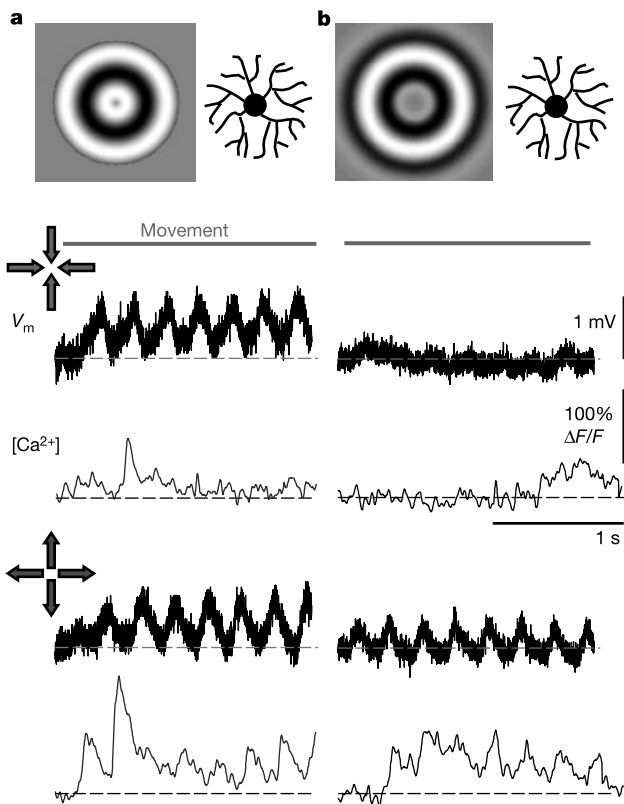


**Figure 7** Responses to expanding and contracting waves. **a**, Somatic voltage ( $V_m$ ) and dendritic  $[Ca^{2+}]$  responses to stimuli comprising an expanding or contracting concentric sinusoidal wave (see Methods). **b**, A different cell excited by a stimulus similar to the one in **a** but with constant intensity in the central part of the stimulus and smoothed transitions between annulus and background. Icons next to stimuli represent relative size of cells.

intensity. To avoid exciting such input we modified the stimuli, with their centre intensity now kept constant (Fig. 7b). With these stimuli the net electrical depolarizations for expanding and contracting motion were small and not systematically different (expanding:  $0.24 \pm 0.06$ ; contracting:  $0.23 \pm 0.05$  mV; ratios:  $0.97 \pm 0.14$ , range: 0.28 to 2.09;  $n = 13$ ; six cells). The expanding stimulus evoked, however, a larger modulation of the membrane potential than the contracting stimulus (expanding:  $V_{rms} = 0.25 \pm 0.06$  mV; contracting:  $V_{rms} = 0.18 \pm 0.04$  mV; ratios:  $1.52 \pm 0.17$ , range 1.08 to 3.38). Although the average ratio is significantly larger than one and we never found the contracting stimulus leading to a larger modulation, the difference between the expanding and contraction stimulus responses was sometimes small. The most likely reason is insufficient centring of the central grey area, leading to residual modulation of the proximal inputs.

The lack of direction-dependent differences in the d.c. (net) responses suggests that the net synaptic input current to the starburst cell is not direction-selective. The alternating current (a.c.) potential evoked by stimuli moving in the preferred direction might, however, generate a direction-selective net  $[Ca^{2+}]$  signal by rectification, which occurs inevitably owing to the nonlinear dependence of calcium influx on the membrane voltage. This suggests that the dendritic branches of starburst cells perform the nonlinear computation required<sup>27</sup> for detection of directed motion.

**Discussion**

It has been proposed that direction selectivity in starburst cell dendrites could arise solely from intrinsic dendritic properties and the asymmetrical arrangement of its input and output synapses<sup>4,21</sup>. In such a model, a stimulus moving in the centrifugal direction first

generates, when passing the proximal part of the dendrite, a depolarizing potential. As this potential spreads electrotonically to the distal dendrite it does so with a temporal delay that allows it to sum with the depolarization directly evoked there by the stimulus, which reaches that part of the cell at a slightly later time. A stimulus moving in the opposite direction excites the distal dendrite first and then later the proximal dendrite. This causes the direct response in the distal dendrite and the electrotonic potential that spreads there from its proximal site of generation to be out of phase and not effectively summed. Hence the peak depolarization in the distal dendrite, which is the region that contains the output synapses, would be smaller for centripetal than centrifugal movement. By the same reasoning, however, we expect strong summation at proximal sites of direct and electrotonically spreading signals for centripetal stimuli. This, however, is not what our circular wave stimuli show.

Thus a simple electrotonic model appears to be inconsistent with our observations. It therefore seems necessary to involve other elements such as active membrane conductances<sup>21,28</sup>, cholinergic (acetylcholine-mediated) connections between amacrine cells<sup>5,29</sup>, or inhibition<sup>4</sup>. Inhibitory inputs are present on starburst cells, as evident from physiological (Figs 2–4, and refs 24, 30) and histochemical<sup>31</sup> data. Our observation that  $[Ca^{2+}]$  signals remain direction-selective in the presence of GABA<sub>A</sub> blockers shows that GABA<sub>A</sub> receptors are not necessary. Although there is also a report that blocking GABA<sub>C</sub> receptors in addition to GABA<sub>A</sub> receptors does not further affect direction selectivity at the ganglion cell level<sup>25</sup>, these results do not definitively rule out a role of GABA<sub>C</sub> at the starburst cell level.

How is the directional motion information used after it has been generated in the starburst cell dendrite? Starburst amacrine cells contain and release GABA and acetylcholine (ACh)<sup>32–34</sup>. There is no direct evidence that GABA release is direction-selective, but we do know that GABA is released upon membrane depolarization<sup>35</sup>, probably using GABA transporters. Net GABA release might be direction-selective (via a rectification mechanism akin to that for calcium influx), because transporter flux is a strongly nonlinear function of membrane voltage<sup>36</sup> and dendritic membrane voltage is predominantly modulated by centrifugal motion (see Fig. 7b). Such a scenario is consistent with previous findings that DS ganglion cells receive asymmetrical inhibition<sup>8</sup> that is mediated by GABA<sub>A</sub> receptors<sup>25,26</sup>. We also believe that the actual data in ref. 9 are consistent with asymmetrical inhibition originating presynaptically.

Direction-selective ACh release should occur since its release is vesicle-based and calcium-dependent<sup>35</sup>. The strong supralinear (about 4th power<sup>37</sup>)  $[Ca^{2+}]$  dependence of vesicular release may thereby further enhance the substantial direction selectivity already present in the  $[Ca^{2+}]$  responses. There have been, however, somewhat conflicting reports on the effect of ACh antagonists on direction selectivity in DS ganglion cells. Responses to moving-bar stimuli are uniformly reduced but direction discrimination appears to be undiminished<sup>7,38–40</sup>. For responses to moving gratings and textures, direction selectivity appears to be abolished<sup>41</sup> by ACh antagonists. These observations suggest that the cholinergic pathway is clearly not the only way for direction information to reach DS ganglion cells; yet cholinergic input (which only originates<sup>42</sup> from starburst cells) to DS ganglion cells conveys directional information, at least for some stimulus types. Excitatory cholinergic inputs may cooperate with inhibitory inputs onto DS ganglion cells in a ‘push–pull’ configuration, with inhibitory input active during null-direction motion and excitatory inputs active during preferred-direction motion. Such a balanced arrangement would not only increase sensitivity but also serve to attenuate the ‘common mode’ response to mere changes in the mean intensity (see also ref. 43).

We still need to know why GABA blockers<sup>25,26</sup> but not acetylcholine blockers<sup>7,38–40</sup> abolish moving-bar direction selectivity. Moving bar stimuli impart a strong overall common-mode intensity change on the cell. Because removal of inhibition disrupts the

common-mode suppression afforded by the push-pull arrangement, it is conceivable that direction selectivity is masked by an increased spiking response to the overall intensity-change (which occurs in both preferred- and null-directions). Cholinergic block, on the other hand, removes excitatory drive. This would reduce the rate of spike production, but it would not eliminate directional selectivity by masking the difference in the responses to null and preferred stimuli.

Direction-selective release of ACh and/or GABA fits well within presynaptic models of direction selectivity<sup>44</sup>. Rather specific wiring between starburst cell and DS ganglion cell dendrites is, however, required. If DS ganglion cells were to indiscriminately contact all starburst cell dendrites within their dendritic field they would receive direction-selective input for all directions, the sum of which would no longer be direction-selective (though it might still be motion sensitive<sup>7</sup>). Therefore, to use the direction-selective output of starburst cells DS ganglion cells have to contact selectively only that subset of dendrites that provides the 'correct' information. To achieve this, a DS ganglion cell dendrite has to receive excitatory cholinergic input from only those starburst cell branches with somata located on the preferred side of the ganglion cell (the side from which a preferred-direction stimulus approaches) and/or GABA-mediated inhibitory input from those branches with somata on the null side of the DS ganglion cell.

An asymmetric connectivity pattern might also account for the non-discriminatory zone found universally in DS ganglion cells<sup>45</sup> because, owing to the distal location of the outputs, motion information in the starburst cell is shifted peripherally. Hence, for inputs located at the preferred-direction edge of the DS ganglion-cell dendritic field the inhibitory outputs of the starburst cell would be shifted beyond the reach of the DS ganglion cell, whereas the excitatory outputs could connect, locally disrupting the balanced push-pull arrangement. Future measurement of excitatory and inhibitory synaptic currents in the DS ganglion cell for stimuli in the non-discriminatory zone should resolve this issue.

Whatever detailed mechanisms of direction detection in the retina eventually emerge, our results demonstrate that branch-specific dendritic computation does occur in the retina and that direction selectively is computed at a stage presynaptic to ganglion cells with the starburst cell dendrites showing behaviour expected for a Reichardt correlation detector<sup>27</sup>. □

## Methods

### Tissue and electrical recordings

Dark-adapted adult albino rabbits were deeply anesthetized with ketamine (Parke-Davis) and xylazine (Bayer), intramuscularly, and then killed with an intravenously applied overdose of pentobarbital (Narcoren; Merial). The eyes were enucleated and the retinas were dissected out under dim red illumination. A piece of mid-peripheral, flat-mounted retina was placed under the microscope and perfused with warmed (~36 °C), oxygenized (95% O<sub>2</sub>, 5% CO<sub>2</sub>) Ames medium (Sigma). The tissue was counterstained with sulphorhodamine 101 dye (Sigma) that allowed us visually to identify with a high success rate (~90%) ON starburst amacrine cells, located in the ganglion cell layer, which were then penetrated using sharp micro-electrodes (filled with 0.2 M K-acetate; 100–250 MΩ; borosilicate with filament, of outer diameter, 1.0 mm and inner diameter 0.58 mm; Clark, Harvard Apparatus, pulled on a P2000 laser puller, Sutter Instruments). First, the voltage (V<sub>m</sub>) response to the visual stimuli was recorded, and the cell was filled with the calcium indicator Oregon Green 488 BAPTA-1 (pipette concentration 5 mM in 0.2 M K-acetate; Molecular Probes). Then, the electrode was carefully retracted and the cell was given about 20–30 min to recover in sulphorhodamine-free medium before calcium imaging started. The GABA<sub>A</sub> receptor antagonists bicuculline and SR-95531 were purchased from Sigma and applied with the extracellular medium.

### Multi-photon calcium imaging

An upright multi-photon microscope (custom in-house design, software developed at Bell Labs by R. Stepanoski and modified at the Max Planck Institute for Medical Research by M. Müller) was used to image calcium signals from selected dendrites<sup>16</sup>. A mode-locked Ti:sapphire laser (Mira-900; Coherent) tuned to 930 nm was used as an excitation source. The scanning laser beam caused only moderate and quickly adapting photoreceptor excitation, allowing us to visually stimulate and optically record calcium signals simultaneously. Filters in the stimulation light path (600 BP 20) and in front of the detector (520 BP 30) ensured that stimulus light did not interfere with fluorescence detection. Image series (64 × 8 pixel images at 62.5 Hz) or line scans (64 pixel lines at

500 Hz) were acquired from short dendritic segments (using water immersion lenses from Zeiss, 63 × 0.9 NA (numerical aperture); or Leica, 60 × 0.9 NA) and analysed off-line (IgorPro; Wavemetrics). While the observed changes in fluorescence suggest changes in [Ca<sup>2+</sup>] of several hundred nM no attempt was made at absolute quantification because no information is available on the endogenous calcium buffer capacity of starburst dendrites.

### Light stimulation

The light stimuli, generated by custom-written software, were output through a video projector (Astrobeam 530; A + K, Germany), and focused through a substage condenser lens (Zeiss 0.32 NA) onto the photoreceptors. The stimulus intensity ranged from about 130 to 2,000 photons s<sup>-1</sup> μm<sup>-2</sup>, roughly covering the mesopic range; stimulus contrasts were between 70 and 87%. The velocity for moving stimuli (bars, gratings) ranged from 500 to 1,300 μm s<sup>-1</sup>. 'Pie-wedge'-shaped sector stimuli (see Figs 2, 3) illuminated 60° sectors of either the cell's dendritic arbor (central sectors) or the near surround (annular surround sectors) for 200 or 400 ms. 'Bull's eye' stimuli (see Fig. 7) consisted of expanding or contracting concentric sinusoidal waves that were centred on the cell and scaled to cover the dendritic field (about 1.5 cycles per cell's radius moving at 3–4 cycles s<sup>-1</sup>). Stimuli were repeated 3–6 times in random order.

### Data analysis

Fluorescence (F) data were spatially averaged over selected regions of interest (ROI) and temporally filtered (box car; image series: 11 frames = 176 ms; line scans, 25 ms).

After background subtraction ΔF/F was calculated for each stimulus presentation. To quantify V<sub>m</sub> and ΔF/F responses the area under the data traces for a defined interval (between t<sub>1</sub> and t<sub>2</sub>) was calculated:

$$a = \int_{t_1}^{t_2} (\Delta F/F) dt$$

Several results for the same stimulus condition were averaged. A directionality vector was calculated as follows:

$$\mathbf{v} = [(a_{+x} - a_{-x})\mathbf{e}_x + (a_{+y} - a_{-y})\mathbf{e}_y] / (a_{+x} + a_{-x} + a_{+y} + a_{-y})$$

where e<sub>x,y</sub> are unit vectors. For each [Ca<sup>2+</sup>] measurement location and for the membrane voltage the value of the directional preference index

$$\text{DPI} = |\mathbf{v}| = \sqrt{(a_{+x} - a_{-x})^2 + (a_{+y} - a_{-y})^2} / (a_{+x} + a_{-x} + a_{+y} + a_{-y})$$

was then calculated. The DPI, for which 0 ≤ DPI ≤ 1 holds, is a measure of directional asymmetry but does not indicate the direction that is preferred. We therefore also used a centrifugality index (CI = cos(α)), with the angle α between the radial direction and v), which indicates whether centrifugal (CI > 0) or centripetal (CI < 0) motion was preferred. Voltage responses to 'Bull's eye' stimuli were fitted with a sum of a constant plus a sinusoidal wave to quantify d.c. depolarization and modulation. For 'Bull's eye'-evoked [Ca<sup>2+</sup>] responses the average ΔF/F was determined.

Received 2 April; accepted 17 June 2002; doi:10.1038/nature00931.

Published online 4 August 2002.

- Barlow, H. B., Hill, R. M. & Levick, W. R. Rabbit retinal ganglion cells responding selectively to direction and speed of image motion in the rabbit. *J. Physiol.* **173**, 377–407 (1964).
- Vaney, D. I., He, S., Taylor, W. R. & Levick, W. R. in *Motion Vision—Computational, Neural, and Ecological Constraints* (eds Zanker, J. M. & Zeil, J.) (Springer, Berlin, 2001).
- Masland, R. H., Mills, J. W. & Cassidy, C. The functions of acetylcholine in the rabbit retina. *Proc. R. Soc. Lond. B* **223**, 121–139 (1984).
- Borg-Graham, L. J. & Grzywacz, N. M. in *Single Neuron Computation* (eds McKenna, T., Zornetzer, S. F. & Davis, J. L.) 347–375 (Academic, London, 1992).
- Famiglietti, E. V. Synaptic organization of starburst amacrine cells in rabbit retina: analysis of serial thin sections by electron microscopy and graphic reconstruction. *J. Comp. Neurol.* **309**, 40–70 (1991).
- Tauchi, M. & Masland, R. H. The shape and arrangement of the cholinergic neurons in the rabbit retina. *Proc. R. Soc. Lond. B* **223**, 101–191 (1984).
- He, S. & Masland, R. H. Retinal direction selectivity after targeted laser ablation of starburst amacrine cells. *Nature* **389**, 378–382 (1997).
- Borg-Graham, L. J. The computation of directional selectivity in the retina occurs presynaptic to the ganglion cell. *Nature Neurosci.* **4**, 176–183 (2001).
- Taylor, W. R., He, S., Levick, W. R. & Vaney, D. I. Dendritic computation of direction selectivity by retinal ganglion cells. *Science* **289**, 2347–2350 (2000).
- Yoshida, K. et al. A key role of starburst amacrine cells in originating retinal directional selectivity and optokinetic eye movement. *Neuron* **30**, 771–780 (2001).
- Euler, T. & Denk, W. Dendritic processing. *Curr. Opin. Neurobiol.* **11**, 415–422 (2001).
- Denk, W., Strickler, J. H. & Webb, W. W. Two-photon laser scanning fluorescence microscopy. *Science* **248**, 73–76 (1990).
- Ehinger, B., Zucker, C. L., Bruun, A. & Adolph, A. *In vivo* staining of oligodendroglia in the rabbit retina. *Glia* **10**, 40–48 (1994).
- Miller, R. F. et al. Structure and functional connections of presynaptic terminals in the vertebrate retina revealed by activity-dependent dyes and confocal microscopy. *J. Comp. Neurol.* **437**, 129–155 (2001).
- Brandon, C. Cholinergic neurons in the rabbit retina: dendritic branching and ultrastructural connectivity. *Brain Res.* **426**, 119–130 (1987).
- Denk, W. & Detwiler, P. B. Optical recording of light-evoked calcium signals in the functionally intact retina. *Proc. Natl Acad. Sci. USA* **96**, 7035–7040 (1999).
- Bloomfield, S. A. Relationship between receptive and dendritic field size of amacrine cells in the rabbit retina. *J. Neurophys.* **68**, 711–725 (1992).
- Taylor, W. R. & Wässle, H. Receptive field properties of starburst cholinergic amacrine cells in the rabbit retina. *Eur. J. Neurosci.* **7**, 2300–2321 (1995).

19. Peters, B. N. & Masland, R. H. Responses to light of starburst amacrine cells. *J. Neurophysiol.* **75**, 469–480 (1996).
20. Miller, R. F. & Bloomfield, S. A. Electroanatomy of a unique amacrine cell in the rabbit retina. *Proc. Natl Acad. Sci. USA* **80**, 3069–3073 (1983).
21. Poznanski, R. R. Modelling the electrotonic structure of starburst amacrine cells in the rabbit retina: a functional interpretation of dendritic morphology. *Bull. Math. Biol.* **54**, 905–928 (1992).
22. Taylor, W. R. & Wässle, H. Receptive field properties of starburst cholinergic amacrine cells in the rabbit retina. *Eur. J. Neurosci.* **7**, 2308–2321 (1995).
23. Pan, Z. H. & Lipton, S. A. Multiple GABA receptor subtypes mediate inhibition of calcium influx at rat retinal bipolar cell terminals. *J. Neurosci.* **15**, 2668–2679 (1995).
24. Linn, D. M. & Massey, S. C. GABA inhibits ACh release from the rabbit retina: a direct effect or feedback to bipolar cells? *Vis. Neurosci.* **8**, 97–106 (1992).
25. Massey, S. C., Linn, D. M., Kittila, C. A. & Mirza, W. Contributions of GABAA receptors and GABAC receptors to acetylcholine release and directional selectivity in the rabbit retina. *Vis. Neurosci.* **14**, 939–948 (1997).
26. Wyatt, H. J. & Daw, N. W. Specific effects of neurotransmitter antagonists on ganglion cells in rabbit retina. *Science* **191**, 204–205 (1976).
27. Reichardt, W. in *Sensory Communication* (ed. Rosenblith, W. A.) 377–390 (MIT Press/Wiley, New York, 1961).
28. Velte, T. J. & Miller, R. F. Spiking and nonspiking models of starburst amacrine cells in the rabbit retina. *Vis. Neurosci.* **14**, 1073–1088 (1997).
29. Keyser, K. T. *et al.* Amacrine, ganglion, and displaced amacrine cells in the rabbit retina express nicotinic acetylcholine receptors. *Vis. Neurosci.* **17**, 743–752 (2000).
30. Zhou, Z. J. & Fain, G. L. Neurotransmitter receptors of starburst amacrine cells in rabbit retinal slices. *J. Neurosci.* **15**, 5334–5345 (1995).
31. Wässle, H., Koulen, P., Brandstätter, J. H., Fletcher, E. L. & Becker, C. M. Glycine and GABA receptors in the mammalian retina. *Vision Res.* **38**, 1411–1430 (1998).
32. Masland, R. H., Mills, J. W. & Hayden, S. A. Acetylcholine-synthesizing amacrine cells: identification and selective staining by using radioautography and fluorescent markers. *Proc. R. Soc. Lond. B* **223**, 79–100 (1984).
33. Brecha, N., Johnson, D., Peichl, L. & Wässle, H. Cholinergic amacrine cells of the rabbit retina contain glutamate decarboxylase and gamma-aminobutyrate immunoreactivity. *Proc. Natl Acad. Sci. USA* **85**, 6187–6191 (1988).
34. Vaney, D. I. & Young, H. M. GABA-like immunoreactivity in cholinergic amacrine cells of the rabbit retina. *Brain Res.* **438**, 369–373 (1988).
35. O'Malley, D. M., Sandell, J. H. & Masland, R. H. Co-release of acetylcholine and GABA by the starburst amacrine cells. *J. Neurosci.* **12**, 1394–1408 (1992).
36. Schwartz, E. A. Depolarization without calcium can release gamma-aminobutyric acid from a retinal neuron. *Science* **238**, 350–355 (1987).
37. Dodge, F. A. Jr & Rahamimoff, R. Co-operative action a calcium ions in transmitter release at the neuromuscular junction. *J. Physiol.* **193**, 419–432 (1967).
38. Ariel, M. & Daw, N. W. Pharmacological analysis of directionally sensitive rabbit retinal ganglion cells. *J. Physiol.* **324**, 161–185 (1982).
39. Grzywacz, N. M., Tootle, J. S. & Amthor, F. R. Is the input to a GABAergic or cholinergic synapse the sole asymmetry in rabbit retinal directional selectivity? *Vis. Neurosci.* **14**, 39–54 (1997).
40. Kittila, C. A. & Massey, S. C. Pharmacology of directionally selective ganglion cells in the rabbit retina. *J. Neurophysiol.* **77**, 675–689 (1997).
41. Grzywacz, N. M., Merwine, D. K. & Amthor, F. R. Complementary roles of two excitatory pathways in retinal directional selectivity. *Vis. Neurosci.* **15**, 1119–1127 (1998).
42. Masland, R. H. & Mills, J. W. Autoradiographic identification of acetylcholine in the rabbit retina. *J. Cell Biol.* **83**, 159–178 (1979).
43. Borst, A. & Egelhaaf, M. Direction selectivity of blowfly motion-sensitive neurons is computed in a two-stage process. *Proc. Natl Acad. Sci. USA* **87**, 9363–9367 (1990).
44. Vaney, D. I., Collins, S. P. & Young, H. M. in *Neurobiology of the Inner Retina* (eds Weiler, R. & Osborn, N. N.) 157–168 (Springer, Berlin, 1989).
45. Barlow, H. B. & Levick, W. R. The mechanism of directionally selective units in rabbit's retina. *J. Physiol.* **178**, 477–504 (1965).

## Acknowledgements

We thank A. Borst and D. Margolis for useful discussions, R. Friedrich for comments on the manuscript, and M. Müller, J. Tritthart and J. Sawinski for technical help.

## Competing interests statement

The authors declare competing financial interests: details accompany the paper on *Nature's* website (<http://www.nature.com/nature>).

Correspondence and requests for materials should be addressed to T.E. (e-mail: [teuler@mpimf-heidelberg.mpg.de](mailto:teuler@mpimf-heidelberg.mpg.de)).